

3D FINITE ELEMENT STUDY OF DAMAGE EVOLUTION IN PARTICLE REINFORCED COMPOSITE

Leon Mishnaevsky Jr. ^{1,2}

(1) University of Stuttgart, IMWF, Pfaffenwaldring 32,
D-70569 Stuttgart, Germany

(2) Institute of Mechanics IV,
Darmstadt University of Technology, Germany

Email: mishnaevsky@web.de

Abstract

3D FE (finite element) simulations of the deformation and damage evolution of SiC particle reinforced Al composites are carried out for different microstructures of the composites. A program for the automatic generation and the design of FE meshes for different 3D microstructures of composites is developed. Numerical testing of composites with random, regular, clustered and gradient arrangements of spherical particles is carried out. The fraction of failed particles and the tensile stress-strain curves were determined numerically for each of the microstructures. It was found that the rate of damage growth increases in the following order: gradient < random < regular < clustered.

Generation of 3D Microstructures and Mesh Design

The optimal design of particle-reinforced materials on the basis of computational simulations of their behaviour has attracted growing interest of researchers over the last two decades [1-9]. The computational design of materials for industrial needs is possible, if the computational difficulties [1, 7] concerning simulation of complex materials at many scale levels are resolved and corresponding technologies for the production of the materials are available. By testing some typical idealized microstructures of a material in numerical experiments, one can determine directions of the material optimization and preferable microstructures of the material under given service conditions.

The purpose of this work was (1) to develop computational tools for the numerical testing of different artificial microstructures of composites (first of all, a simple and efficient method of automated generation of artificial microstructures and the mesh design for these microstructures, as well as subroutines for the damage simulation), and (2) to analyse the effect of microstructures of particle-reinforced metal matrix composites on the deformation and damage resistance by carrying out 3D numerical experiments.

In order to generate and mesh 3D artificial microstructures of the composites, a new program "Meso3D" [10] for the automatic design of three-dimensional FE meshes for particle-reinforced materials with different particle arrangements, shapes and types of localization (clustered, gradient), was developed (Figure 1). The program works with the commercial software MSC/PATRAN and produces artificial microstructures (i.e., different arrangements of round and ellipsoidal inclusions in a matrix) on the basis of given parameters and probability distributions of particle coordinates and sizes, and generates the finite element databases for the computational testing of the materials with the required artificial

microstructures. The designed microstructures are meshed with tetrahedral elements using the free meshing technique. Figure 2 shows several examples of generated FE meshes.

The microstructures with the random particles arrangement are generated using the uniform random number generator. The coordinates of the centers of particles for the regular (and any other pre-defined) particles arrangements can be read from a text input file (Figure 1). In order to generate the localized particle arrangements, like clustered, layered and gradient particle arrangements, the coordinates of the particle centers are calculated as random values distributed by the Gauss law. The mean values of the corresponding normal distribution of the coordinates of particle centers are assumed to be the coordinates of a center of a cluster (for the clustered structure), or the Y- or Z- coordinate of the border of the box (for the gradient microstructure). The standard deviations of the distribution can be varied, from highly clustered or highly gradient arrangements (very small deviation) to the fast uniformly random particle arrangements (a deviation comparable with the box size).

Numerical Model and Properties of Phases

Using the program “Meso3D” [10], we simulated the mechanical behavior and damage evolution in the materials with different (artificially designed) microstructures, and determined the amount of failed particles and the tensile stress-strain curves for each of the microstructures.

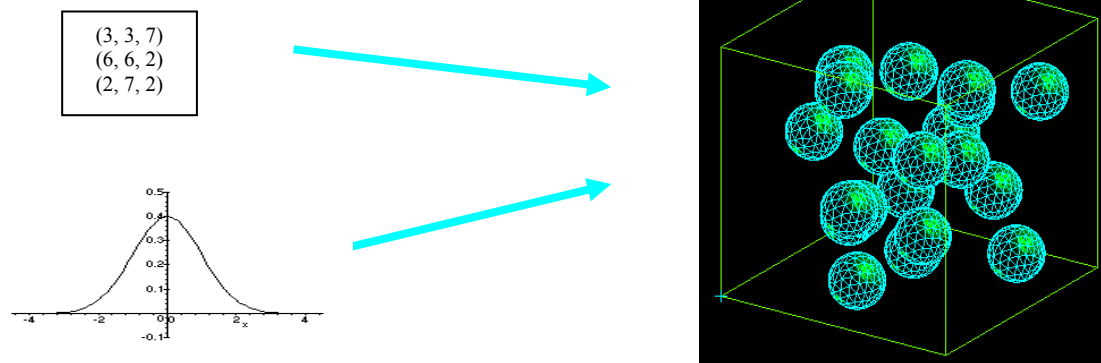


FIGURE 1. Schema of the program “Meso3D”: design of complex FE meshes from probability distributions or coordinate lists.

The problem was solved in the framework of the embedded cell approach [1, 7]. The FE meshes of the composites with different microstructures (a given amount of SiC particles in a box 10 x 10 x 10 mm, filled with elastoplastic Al matrix), generated with the use of the program “Meso3D” and commercial code MSC/PATRAN, were placed in a bigger box 14 x 14 x 14 mm. The embedding zone behaved as a composite with averaged properties, i.e. as an elastic-plastic material. The SiC particles behaved as elastic isotropic damageable solids, characterized by Young modulus $E_p = 485$ GPa, Poisson’s ratio 0.165 and the local damage criterion, discussed below. The Al matrix was modeled as isotropic elasto-plastic solid, with Young modulus $E_M = 73$ GPa, and Poisson’s ratio 0.345. The experimental stress-strain curve for the Al matrix was taken from [14]. The elements in the embedding were assigned the averaged mechanical properties of the Al/SiC composite, with Young modulus $E_{Av} = 75.7$ GPa (for the volume content 10%) and $E_{Av} = 88.4$ GPa (for 15%), and Poisson’s ratio 0.323 taken from [11]. The elasto-plastic stress –strain curve for the composite

(embedding) was taken from [11] as well. When approximating the experimental stress-strain curve by the deformation theory flow relation (Ludwik hardening law) $\sigma_y = \sigma_{yn} + h \varepsilon_{pl}^n$, where σ_y - the actual flow stress, σ_{yn} - the initial yield stress, and ε_{pl} - the accumulated equivalent plastic strain, h and n - hardening coefficient and the hardening exponent, the parameters of the curve are as follows: $\sigma_{yn} = 205$ MPa, $h = 457$ MPa, $n = 0.20$. For the composite (embedding), the parameters were: $\sigma_{yn} = 216$ MPa, $h = 525.4$ MPa, $n = 0.25$. We considered cells with 5, 10 and 15 particles, the volume content of the inclusion phase was 2.5%, 5%, 10% and 15%. Totally, the models contained about 30000 elements. Each particle contained about 400 finite elements. The radii of particles were calculated from the prescribed volume content and particle amount in the box, and were as follows: 1.1676 mm (volume content/VC=10%, N=15), 0.9267 mm (VC=5%, N=15), 1.3365 mm (VC=10%, N=10) and 1.0608 (VC=5%, N=10). The nodes at the upper surface of the box were connected, and the displacement was applied to only one node. The model was subject to the uniaxial tensile displacement loading, 2.0 mm. The uniaxial tensile response of each microstructure was computed by the finite element method. The simulations were done with ABAQUS/Standard.

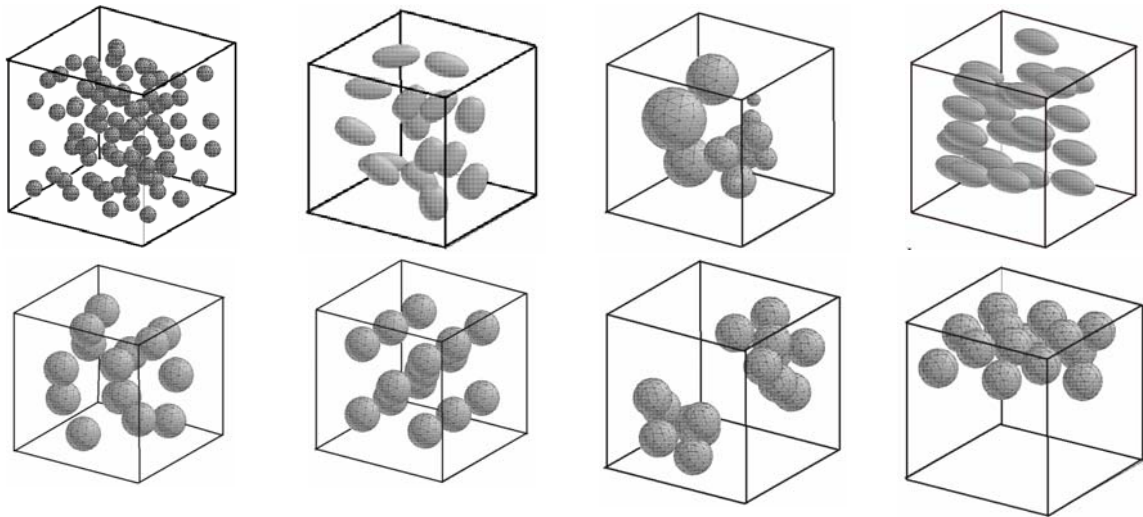


FIGURE 2. Examples of designed FE meshes: random particle arrangement, randomly oriented ellipsoids, round particles of different sizes, aligned ellipsoids (upper row), random, regular, clustered, and highly gradient particle arrangements (lower row).

Only damage in SiC particles was considered at this stage of the work. The damage was modeled using the element weakening technique [6]. The finite elements in which the damage criterion (maximum principal stress) exceeded a critical value, were considered to be failed, and the Young modulus of these elements was set to a very low value (50 Pa). An ABAQUS Subroutine USRFLD, which allows to simulate the local damage growth as a weakening of finite elements was developed. According to [13], the SiC particles in AlSiC composites fail, if the critical maximum principal stress in SiC particle exceeds 1500 MPa. This value was used in our simulations as a criterion of the failure of SiC particles as well. As output parameters of the numerical testing of the microstructures, the effective response of the materials and the amount of failed particles N_F versus the far-field strain curves were considered.

Deformation and damage behavior of composites with the random arrangement of particles

The deformation and damage evolution of the Al/SiC composites with random SiC particle arrangements were simulated with the use of the model described above. The purpose of this part of the investigation was to verify whether the “random” particle arrangements have peculiarities as compared with regular or localized particle arrangements, and whether these peculiarities are stable, reproducible and typical for the random arrangements. Since the random particle arrangements were generated from a pre-defined random number seed parameter (idum), (which should ensures reproducibility of the simulations), variations of this parameter lead to the generation of new microstructures.

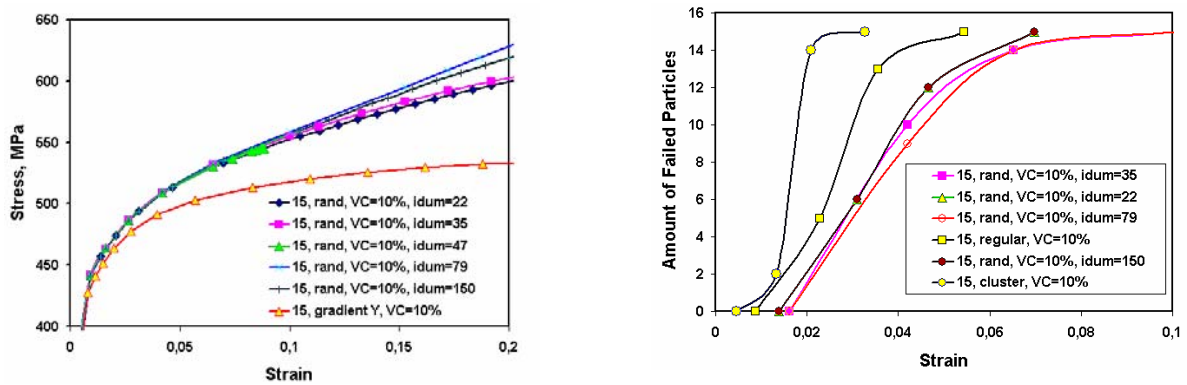


FIGURE 3. Tensile stress-strain curves and the amount of failed particles versus the far-field applied strain curves for the different realisations of the random arrangement

5 realizations of the random microstructures with 15 spherical particles and volume content of ceramic phase 10% (produced with different random numbers seeds) were generated and tested. Figure 3 shows the tensile stress-strain curves for the 5 random arrangements (15 particles, volume content 10%). For comparison, we included also the gradient particle arrangements. Figure 3 shows the amount of failed particles plotted versus the far-field applied strain as well.

One can see from Figure 3, that the effective responses of the materials with random microstructures (even in different realizations) lie very close one to another and differ from that for the regular or localized microstructures. However, some variations of both flow stress and damage behavior of different random microstructures are observed as well, especially, after the far-field strain exceeds 0.1. The difference between the stresses for different realizations of the same random structure falls in the range of 2% even at the rather high far-field strain ($\epsilon=0.2$). For comparison, the difference between the regular and gradient particle arrangement is about 16% at the far-field strain 0.2, and 9% at the far-field strain 0.1 (see Figure 3). Therefore, although the stress-strain curves diverge a little bit when the strain is higher than 0.1, the differences between realizations of the random microstructure are still much smaller, than the difference of the mechanical response between the different types of the microstructures. In the following part, at least three to five realizations of random microstructures will be simulated and averaged, when a random microstructure is compared with other microstructures.

The rate of particle failure is lower for all the considered random particle arrangements than for the regular and clustered microstructures: the fraction of failed particles increases from 40% to 80%, when the far-field strain increases 2.8 times in the case of the random

particle arrangement, and increases from 20% to 86% when the far-field strain increases 1.5 times for the regular particle arrangement.

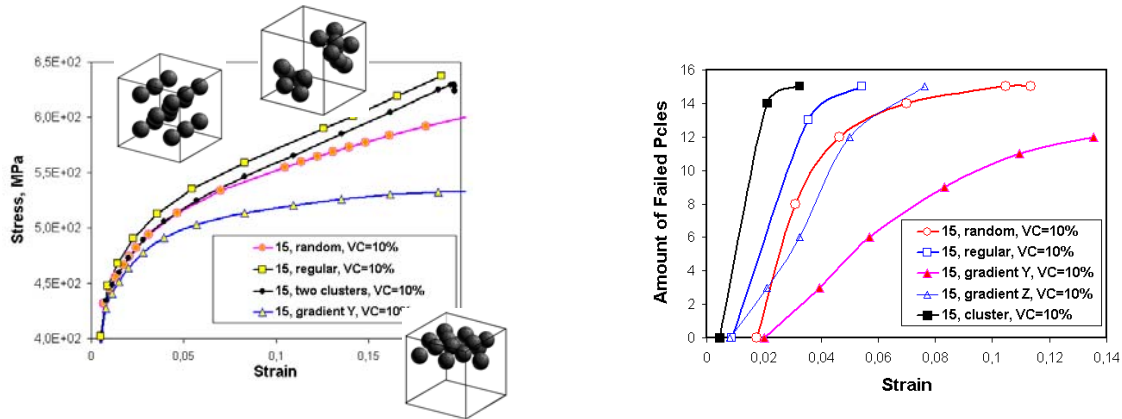


FIGURE 4. Tensile stress-strain curves (left) and the amount of failed particles versus the far-field applied strain curves (right) for the different arrangements of particles (random, regular, clustered and gradient).

Effect of the particle arrangement on the damage evolution in composites

The effects of particles arrangement and localization on the deformation and damage evolution in the composite were considered. Figure 2 (lower row) shows the random, regular, clustered, and highly gradient arrangements of the particles, considered in the simulations. Two types of the gradient particle arrangements were considered: an arrangement of particle with the vector of gradient (from low particle concentration region to a high particle concentration region) coinciding with the loading direction (called in the following a “gradient Y” microstructure), and a microstructure with the gradient vector perpendicular to the loading vector (called in the following “gradient Z” microstructure). The standard deviations of the normal distribution of the Y or Z coordinates of the particle centers (for the Y and Z gradient microstructures, respectively) were taken 2 mm, what ensured rather high degree of gradient. The same standard deviations were taken for the clustered particle arrangements. Figure 4 shows the tensile stress-strain curves and the amount of failed particles in the box plotted versus the far-field applied strain for the random, regular, clustered and gradient microstructures (for 15 particles, VC =10%).

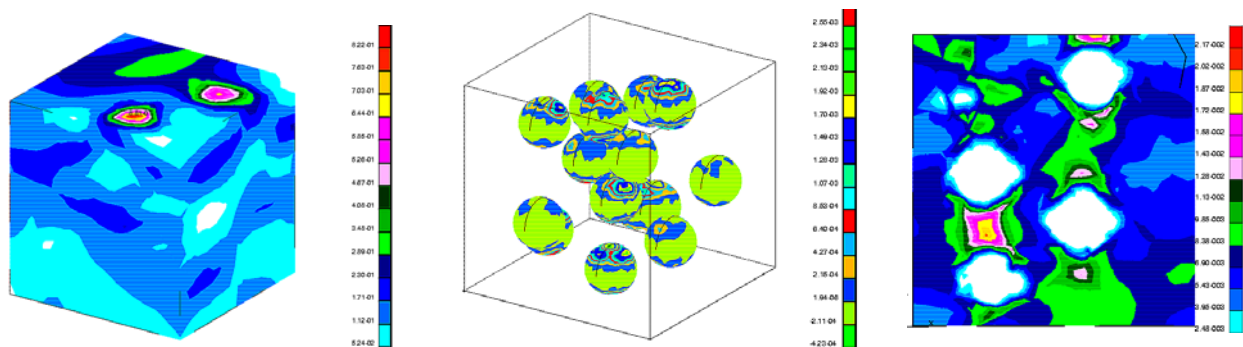


FIGURE 5. Distribution of equivalent plastic strains on box boundary (left), on the particle/matrix interface and in a vertical section in the microstructures with random particle arrangements (15 particles, VC =10%).

Figure 5 gives the distributions of equivalent plastic strains on the boundaries of the microstructure box, on the particle/matrix interfaces and in a vertical section in the microstructures with random particle arrangements (15 particles, VC =10%). Figure 6 shows the von Mises stress distribution in the matrix in the microstructures with 10 particles (VC =10%), with highly gradient and regular particle arrangements.

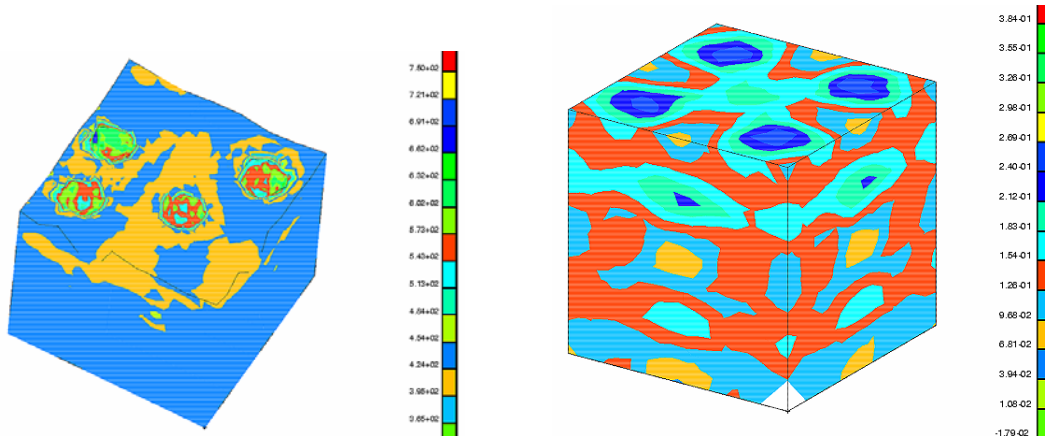


FIGURE 6. Distribution of von Mises stresses in the matrix in the microstructures with highly gradient (left, a horizontal section of the structure) and regular (right) particle arrangements (10 particles, VC =10%).

It can be seen from Figure 4 that the particle arrangement hardly influences the effective response of the material in elastic area or at small plastic deformation. The influence of the type of particle arrangement on the effective response of the material becomes significant only at the load at which the particles begin to fail. However, after the particle failure begins, the effect of particle arrangement increases with increasing the applied load.

After the first particle fail, the flow stress of the composite increases with varying the particle arrangement in the following order: gradient < random < clustered < regular microstructure. One can see from Figure 4 that the rate of damage growth increases in the following order: gradient < random < regular < clustered.

The strength and damage resistance of a composite with a gradient microstructure strongly depends on the orientation of the gradient in relation to the direction of loading. In the case of the microstructure with vertical gradient (along the loading vector), the rate of particle failure is very low (about 6.35 particle/mm) and the particle failure begins at relatively high displacement loading, 0.2 mm. In the case of the microstructure with horizontal gradient (normal to the loading vector), the rate of particle failure is the same as for random microstructures.

Conclusions

Numerical analysis of the effect of microstructure, arrangement and volume content of hard damageable inclusions in plastic matrix on the deformation and damage growth has been carried out. The effect of the particle arrangement on the effective response of the material becomes significant only at the load at which the particles begin to fail. The flow stress of the composite increases with varying the particle arrangement in the following order: highly gradient < random < clustered < regular microstructure. The rate of damage growth increases in the following order: gradient < random < regular < clustered.

Acknowledgement: The author is grateful to the German Research Council (DFG) for its support through the Heisenberg fellowship. The fruitful and interesting discussions with Professor S. Schmauder, and his permanent support and advises are gratefully acknowledged.

References

1. Mishnaevsky Jr, L and Schmauder, S., *Appl. Mechan Reviews*, Vol. 54, 1, 2001, pp. 49-69
2. Mishnaevsky Jr, L., *Damage and Fracture of Heterogeneous Materials*, Balkema, Rotterdam, 1998, 230 pp.
3. Böhm, H. J., and Han, W., (2001), *Modelling Simul. Mater. Sci. Eng.*, 9, 47-65
4. Segurado J, C. González and J. LLorca, *Acta Mater*, Vol. 51, 8, 2003, 2355-236
5. Mishnaevsky Jr, L., N. Lippmann and S. Schmauder, *Int. J. Fracture* 120 (4), 2003, pp. 581-600, *Zeitschrift f. Metallkunde*, 94, 2003, 6
6. Mishnaevsky Jr, L., U. Weber and S. Schmauder, *Int. J. Fracture* (125), 2004. pp. 33–50
7. Mishnaevsky Jr, L. M. Dong, S. Hoenle, S. Schmauder, *Comput Mater Sci.*, (16) 1999, 1-4, 133-143
8. Mishnaevsky Jr, L., *Eng. Fract. Mech.* 56 :1 (1997) 47-56
9. Mishnaevsky Jr, L., Shioya T., *Journ School of Engnrng, Univ. Tokyo*, 48, 2001, pp. 1-13
10. Mishnaevsky Jr L., Program “Meso3D”, <http://www.mpa.uni-stuttgart.de/Verfahrens-entwicklung/schm/leon/meso3d.pdf>
11. Wulf, J., Neue Finite-Elemente-Methode zur Simulation des Duktilbruchs in Al/SiC
Dissertation MPI für Metallforschung, Stuttgart, 1995
12. Hu, G., G. Guo, D. Baptiste. *Comp. Mater. Sci*, 9 (1998) 420-430
13. Derrien K., D. Baptiste, D. Guedra-Degeorges, J. Foulquier, *Int. J. Plasticity*, Vol. 15, 667-685, 1999
14. Soppa, E., Personal communication (2003)

